Experimental and chemical kinetic modeling investigation of methyl butanoate as a component of biodiesel surrogate

Aditya Dilip Lele[a], Sonal K. Vallabhuni[b], Kai Moshammer[b], Ravi X. Fernandes[b], Anand Krishnasamy[a] and Krithika Narayanaswamy[a]

[a]Department of Mechanical Engineering, Indian Institute of Technology Madras, Chennai 600036, India
[b]Physikalisch-Technische Bundesanstalt, Bundesallee 100, 38116 Braunschweig, Germany

Contents

1 Methyl butanoate mechanism reduction

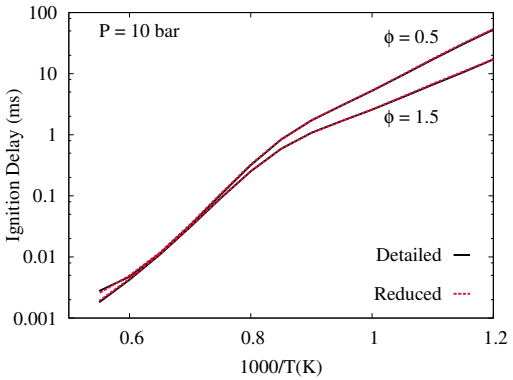

(a) P = 10 bar, ϕ = 0.5, 1.5

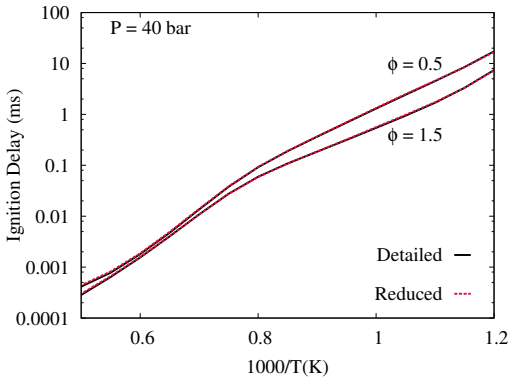

(b) P = 40 bar, ϕ = 0.5, 1.5

Figure S1: Comparison between computed ignition delay times of methyl butanoate/air mixtures between: (i)detailed mechanism[3](Solid lines) comprising 275 species and 1545 reactions and (ii) reduced mechanism(Dashed line) obtained using DRGEP [4] including 89 species and 560 reactions.

2 Additional validations for MB

2.1 RCM

2.1.1 Effect of rate constant uncertainties

Figure S2 shows sensitivity analysis for fuel specific reactions in intermediate temperature range. It shows that the ignition delays are most sensitive to reactions H atom abstraction by HO_2 and CH_3O_2 radicals. Rate constants for these reactions have an uncertainty of a factor of 2.5 [5]. To assess the effect of these uncertainties on ignition delay predictions, ignition delay times in RCM were modeled using extreme ends of this set of rate constants based on the uncertainty. Figure S3 shows the effect of these uncertainties on ignition delay time predictions. These uncertainties can effect the ignition delay predictions in intermediate temperature range from 20–50%

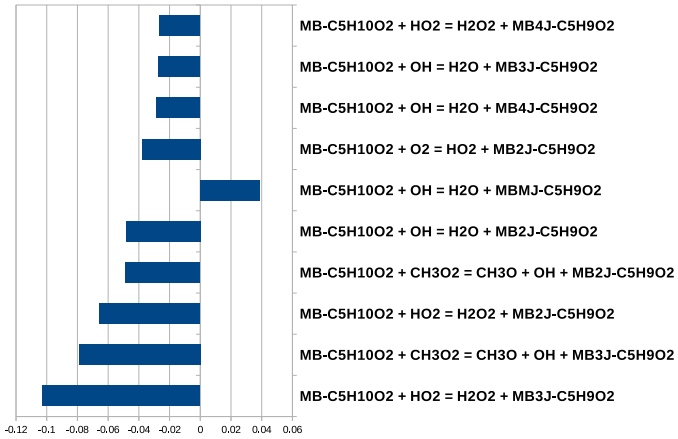

(a) P = 30 bar, ϕ = 0.50, T = 900K

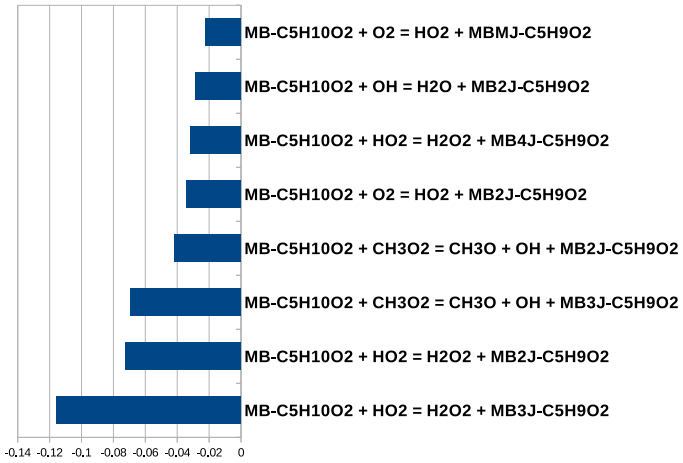

(b) P = 20 bar, ϕ = 1.00, T = 950K

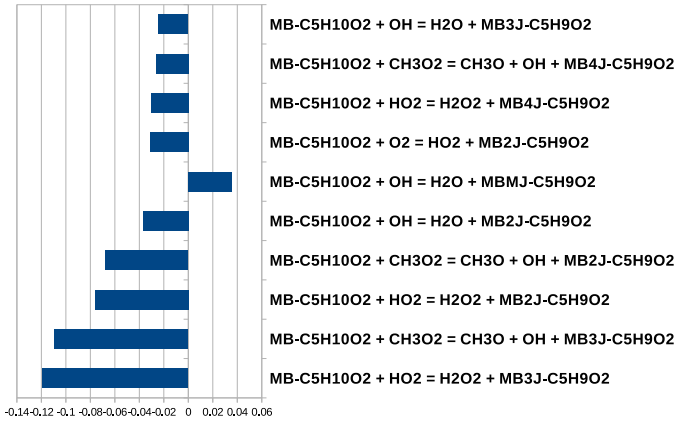

(c) P = 20 bar, ϕ = 1.50, T = 900K

Figure S2: Sensitivity analysis for ignition delays of MB/O_2/Ar mixtures at ϕ = 1.0, P = 4 atm, and T = 1300 K. Sensitivities are determined by multiplying each rate constant by a factor of 2, and finding the corresponding change in ignition delays. Only those reactions involving fuel with sensitivities 0.02 are reported here.

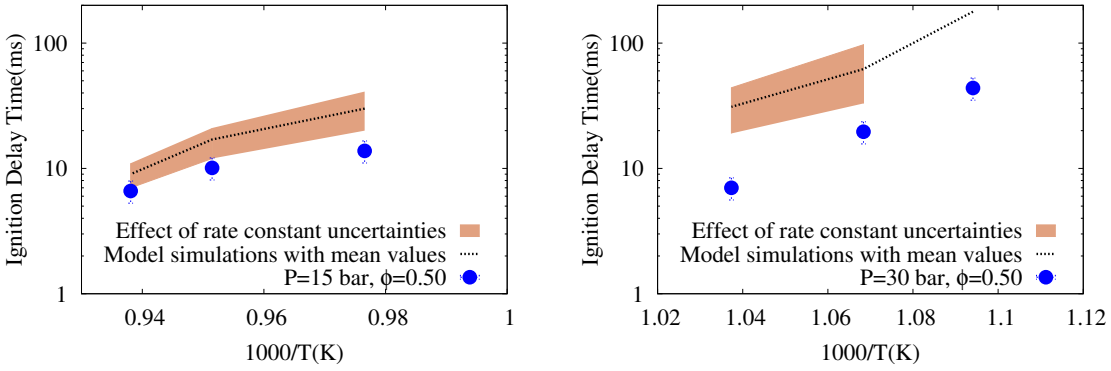

(a) P = 15 bar, ϕ = 0.50

(b) P = 30 bar, ϕ = 0.50

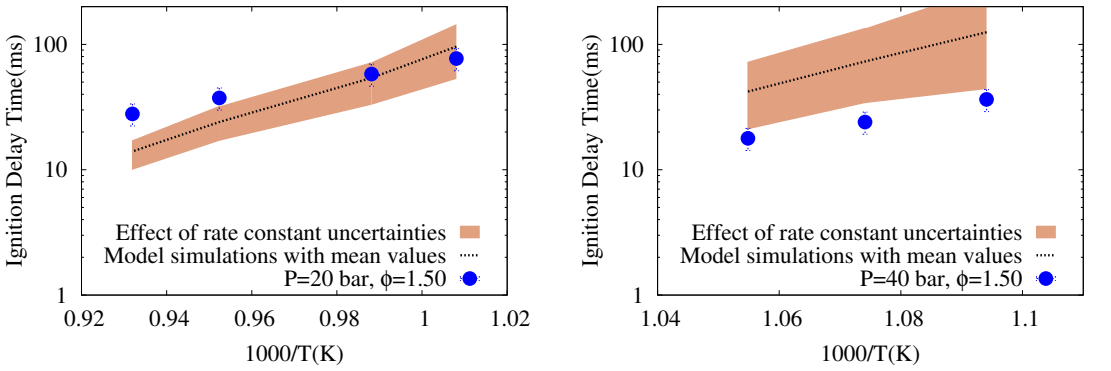

(c) P = 20 bar, ϕ = 1.50

(d) P = 40 bar, ϕ = 1.50

Figure S3: Ignition delays of MB/O_2/diluent mixtures; symbols : experiments from this study; dashed lines: simulations performed with mean values for rate constants of reactions of the reaction classes H abstraction by HO_2 and CH_3O_2; shaded area: effect of uncertainties in rate constant values. Ignition delays are defined based on the time required for maximum rate of pressure rise in the experiments and the same criterion is used in the simulations as well.

2.1.2 Effect of equivalence ratio

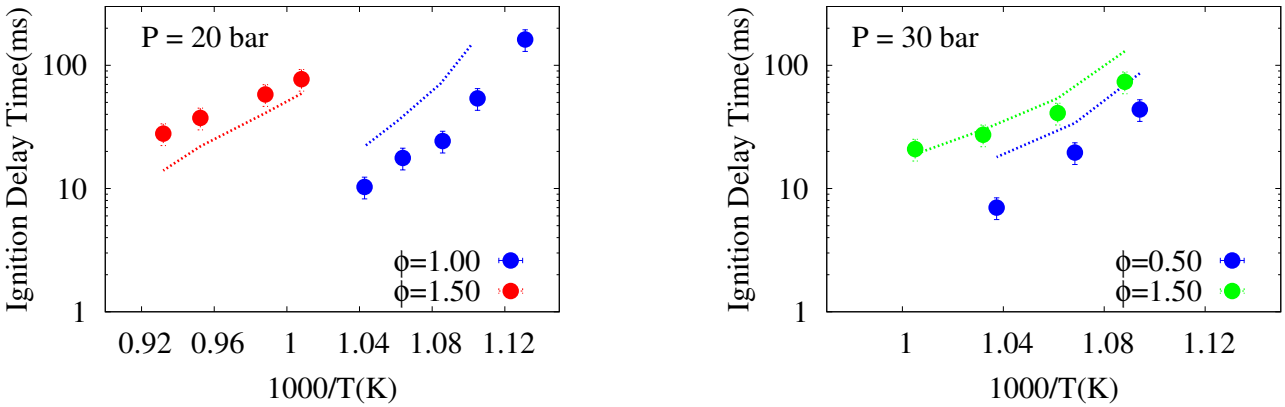

(a) ϕ = 1.00 and ϕ= 1.50

(b) ϕ = 0.50 and ϕ= 1.50

Figure S4: Effect of (a) pressure and (b–d) equivalence ratio on ignition delays; symbols : experiments (this study); lines: simulations. The experimental dataset is same as that presented in Fig. S3, re-plotted to bring out the trends when varying pressure and equivalence ratios.

2.2 Flat flame burner

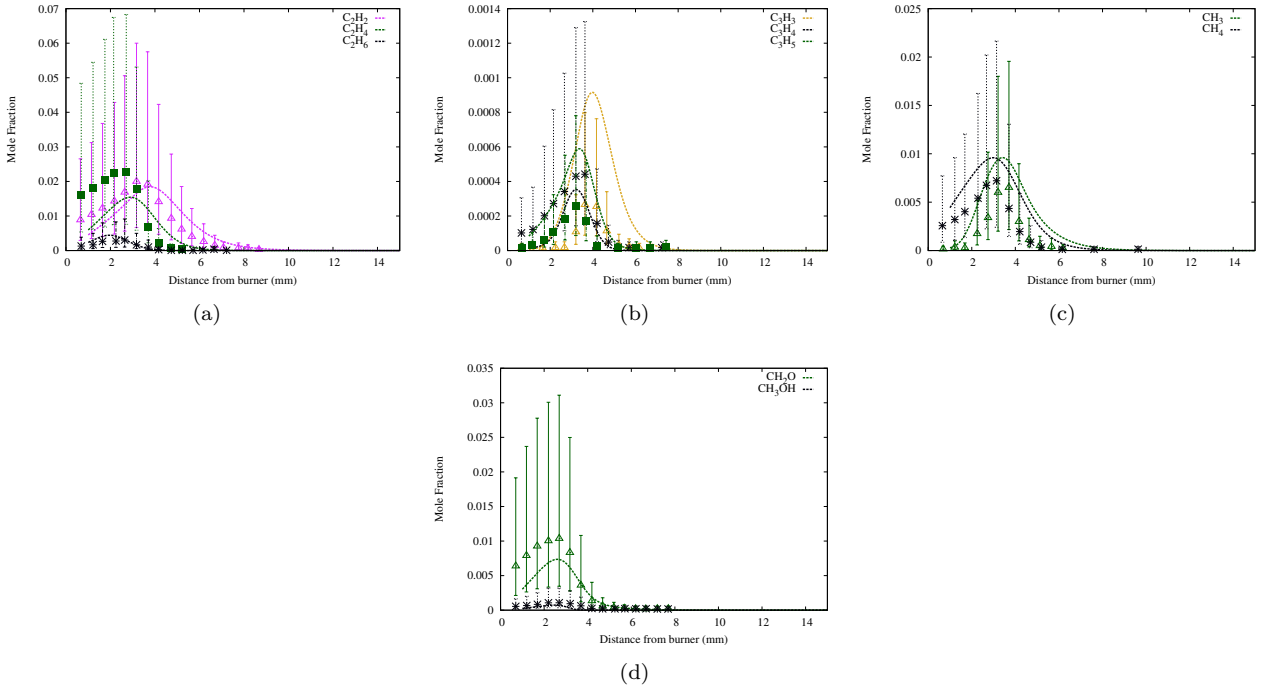

Figure S5: Comparison between simulated and experimental species profiles for a premixed flat flame burner at P = 30 torr, $\phi = 1.56$; symbols: experiments by Yang et al. [6], lines: simulations with IITM high T model. Simulated species profiles have been shifted by 1 mm.

2.3 Counter-flow diffusion flame

Diffusion plays the predominant role in counter-flow diffusion flames. Even though the focus of current study is mainly on the kinetics, this configuration provides a useful test for model validation. Gail et al. [7] measured species concentrations in opposed flow diffusion flame at atmospheric pressure. This data is compared against model simulations in Fig. S6. Model prediction for major species such as fuel (MB), CO and CO_2 are in good agreement with the experimental data, except a minor shift in the peak concentration for the products. In case of minor species, model predicts the concentrations of CH_4, C_2H_4 and C_3H_6 fairly well (within 30%), while matching the position of peak concentrations. The concentration of acetylene is overpredicted, while that of C_3H_6 and C_3H_8 are underpredicted.

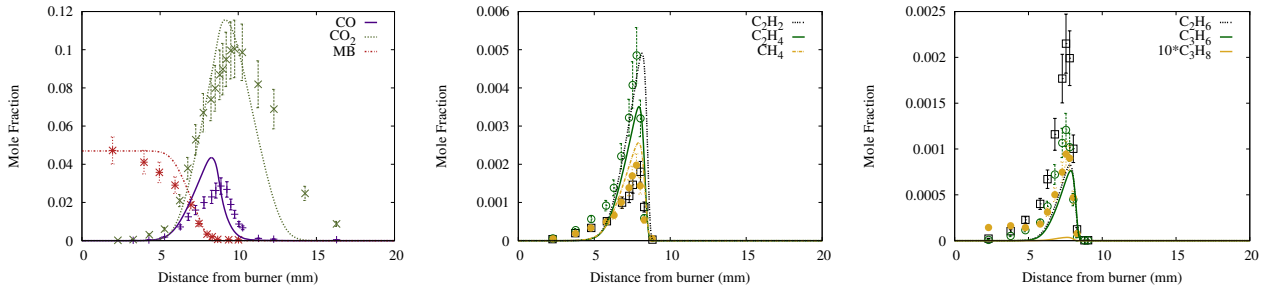

Figure S6: Species concentrations versus distance from burner in a counter-flow diffusion flame. Symbols: experiments [7]; lines: model simulations.

Overall, the model shows a modest agreement for all the flame configurations. Although, flame configurations were not a target for the reduction of the detailed MB mechanism [3], the extent of reduction combined with the revisions introduced to the kinetic model and the the choice of a well validated base chemistry result in the satisfactory results shown by the proposed model for these configurations.

In summary, in this section, the proposed IITM high T reaction mechanism has been assessed in great detail for its kinetic description of methyl butanoate oxidation by comparing it against a wide variety of experimental data. The validation tests conducted in this study show that the IITM high T model is able to capture combustion characteristics of methyl butanoate satisfactorily. The proposed model, capable of describing methyl butanoate and *n*-dodecane kinetics, consists of 283 species and ∼2500 reactions. Thermodynamic data for the species present in the MB sub-mechanism is taken from the reference mechanism [3], while the remaining are taken from Narayanaswamy et al. [1]. THERM [8] is used

to obtain thermodynamic data whenever required. The kinetic model including the complete mechanism, thermodynamic and transport data files are made available with the supplementary materials in ChemKin [9] as well as FlameMaster [10] format.

3 Additional validations for MB kinetic model with low temperature chemistry pathways

3.1 JSR

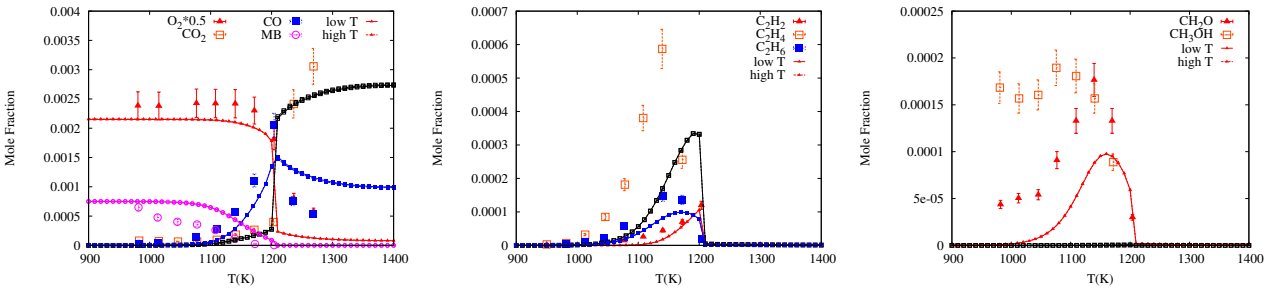

Figure S7: Species concentrations versus initial temperature measured in a JSR at atmospheric condition for ϕ=1.13. Symbols: experimental data from Gail et al. [11]; solid lines with symbols: simulations with MB model including low temperature chemistry; dashed lines with symbols: simulations with MB model including only high temperature chemistry.

3.2 VPFR

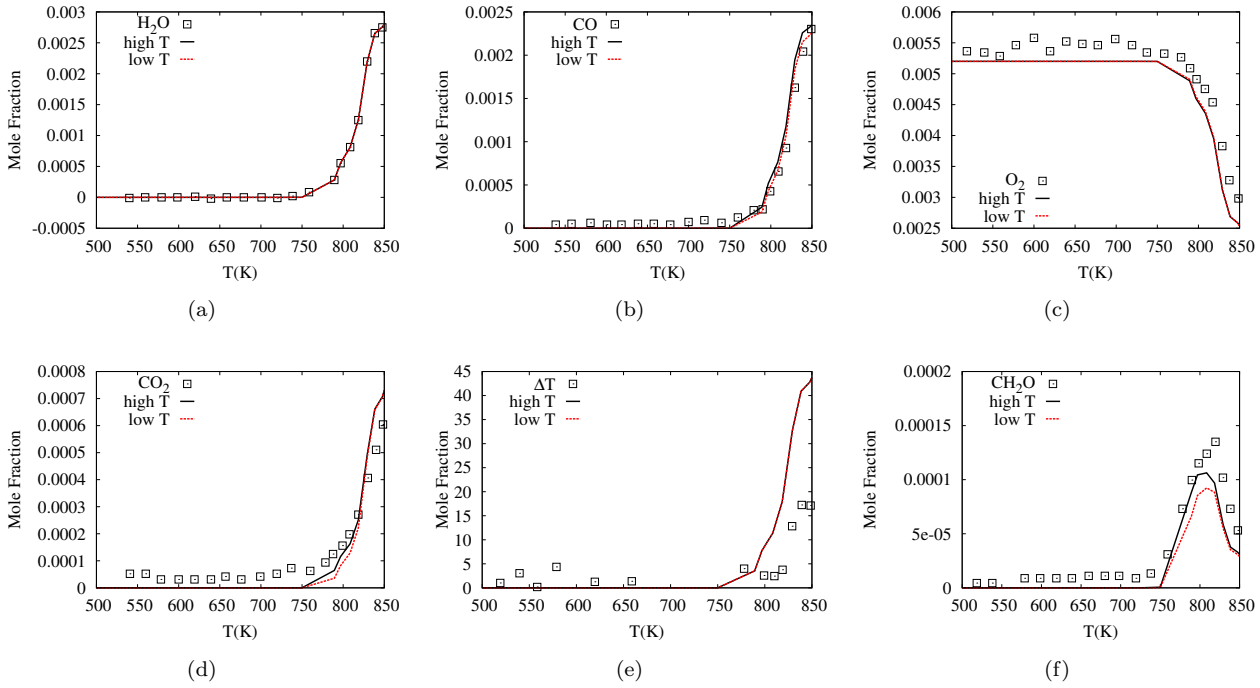

Figure S8: Species concentrations versus initial temperature in Princeton VPFR at P=12.5 atm and ϕ=1. Symbols : experiments from Marchese et al. [12]; lines : simulations.

3.3 Potential NTC region

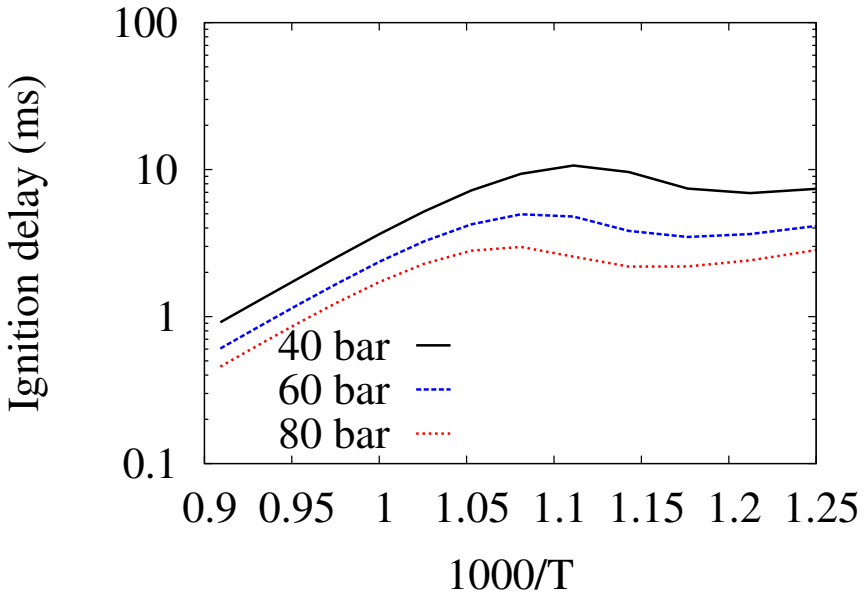

Figure S9: Adiabatic isochor homogeneous reactor computations with *IITM model* (with low-temperature chemistry pathways for MB) indicating potential pressure-temperature range where NTC or two-stage ignition can be observed for methyl butanoate.

4 Validation of combined mechanism with reference DD mechanism [1]

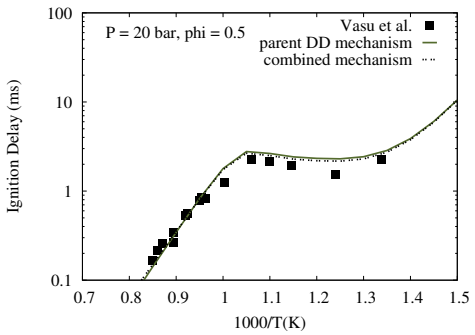

(a) Ignition delay times

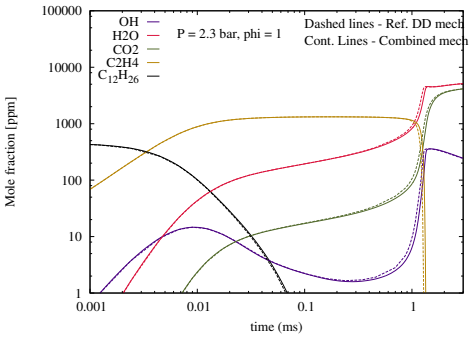

(b) Shock tube species profiles

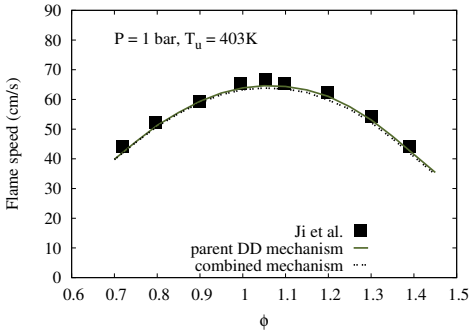

(c) Laminar burning velocities

Figure S10: Comparison between (a) simulations and experiments[13] for ignition delay times of n-dodecane and (b) shock tube species profiles simulations for n-dodecane autoignition and (c) simulations and experiments[14] for laminar burning velocities : (i) parent n-dodecane(DD)[1] mechanism (Solid lines) and (ii) combined methyl butanoate + n-dodecane(DD) mechanism (Dashed lines)

5 Additional reactions incorporated from Huynh et al. [2] submodel

Table 1: List of additional reaction incorporated in the combined mechanism while incorporating Huynh et al. [2] thermal decomposition submodel.

No.	Reaction
1	MP3J-$C_4H_7O_2$ $\leftrightharpoons$ C_2H_4 + CH_3OCO
2	MP3J-$C_4H_7O_2$ $\leftrightharpoons$ MP2D-$C_4H_6O_2$ + H
3	C_3H_6CHO-2-C_4H_7O $\leftrightharpoons$ C_3H_6 + HCO
4	C_3H_6CHO-1-C_4H_7O $\leftrightharpoons$ C_2H_4 + CH_2CHO
5	S-C_3H_5CO + H_2 $\leftrightharpoons$ S-C_3H_5CHO + H
6	S-C_3H_5CO $\leftrightharpoons$ C_3H_5-S-C_3H_5 + CO

6 Species nomenclature

Table 2: Species nomenclature for Methyl butanoate sub-mechanism

Species name in mechanism	Detailed formula
ME2J-C3H5O2	C$^\bullet$-C(=O)-O-C
MEMJ-C3H5O2	C-C(=O)-O-C$^\bullet$
C3H6OOH-3J1-C3H7O2	C-C-C-O-O$^\bullet$
ME2DO-C3H4O3	C(=O)-C(=O)-O-C
C3KET12-C3H6O3	C-C-(O-O-H)C(=O)
C3KET13-C3H6O3	C(O-O-H)-C-C(=O)
C3H6OOH1-2O2-C3H7O4	C-C-(O-O$^\bullet$)C(O-O-H)
C3H6OOH1-3O2-C3H7O4	C(O-O$^\bullet$)-C-C(O-O-H)
S-C3H5CO	C-C=C-C$^\bullet$(=O)
C3H6CHO-2-C4H7O	C-C$^\bullet$-C-C(=O)
C3H6CHO-1-C4H7O	C$^\bullet$-C-C-C(=O)
C2H5CHCO	C-C-C=C(=O)
MP2D2J-C4H5O2	C=C$^\bullet$-C(=O)-O-C
MP2D3J-C4H5O2	C$^\bullet$=C-C(=O)-O-C
MP2DMJ-C4H5O2	C=C-C(=O)-O-C$^\bullet$
MP2D-C4H6O2	C=C-C(=O)-O-C
BAOJ-C4H7O2	C-C-C-C(=O)-O$^\bullet$
MP3J-C4H7O2	C$^\bullet$-C-C(=O)-O-C
MB2D-C5H8O2	C-C=C-C(=O)-O-C
MB2O-C5H9O3	C-C-C(-O$^\bullet$)-C(=O)-O-C
MB3O-C5H9O3	C-C(-O$^\bullet$)-C-C(=O)-O-C
MB2J-C5H9O2	C-C-C$^\bullet$-C(=O)-O-C
MB3J-C5H9O2	C-C$^\bullet$-C-C(=O)-O-C
MB4J-C5H9O2	C$^\bullet$-C-C-C(=O)-O-C
MBMJ-C5H9O2	C-C-C-C(=O)-O-C$^\bullet$
MB-C5H10O2	C-C-C-C(=O)-O-C
MEMDO2J-C3H3O3	C$^\bullet$-C(=O)-O-C(=O)
ME2DOMJ-C3H3O3	C(=O)-C(=O)-O-C$^\bullet$
MP2DO3J-C4H5O3	C$^\bullet$-C(=O)-C(=O)-O-C
MPMDO3J-C4H5O3	C$^\bullet$-C-C(=O)-O-C(=O)
MMMOOH1J-C2H3O4	C$^\bullet$(=O)-O-C(O-O-H)
BAOJ4DO-C4H5O3	C(=O)-C-C-C(=O)-O$^\bullet$
BAOJ3DO-C4H5O3	C-C(=O)-C-C(=O)-O$^\bullet$
MEMOOH2J-C3H5O4	C$^\bullet$-C(=O)-O-C(O-O-H)
MB4O-C5H9O3	C(-O$^\bullet$)-C-C-C(=O)-O-C
MBMO-C5H9O3	C-C-C-C(=O)-O-C(-O$^\bullet$)
MBMJDO-C5H7O3	C-C-C-C(=O)-O-C$^\bullet$(=O)
MB4JDO-C5H7O3	C$^\bullet$(=O)-C-C-C(=O)-O-C
MB3DO-C5H8O3	C-C(=O)-C-C(=O)-O-C
MBMDO-C5H8O3	C-C-C-C(=O)-O-C(=O)
MP3DO2D-C4H4O3	C(=O)-C=C(=O)-O-C
ME2JDO-C3H3O3	C$^\bullet$(=O)-C(=O)-O-C
MB4DO-C5H8O3	C(=O)-C-C-C(=O)-O-C
MB2OOH3J-C5H9O4	C-C$^\bullet$-C(O-O-H)-C(=O)-O-C

MB2OOHMJ-C5H9O4	C-C-C(O-O-H)-C(=O)-O-C$^{\bullet}$
MB3OOH4J-C5H9O4	C$^{\bullet}$-C(O-O-H)-C-C(=O)-O-C
MB3OOHMJ-C5H9O4	C-C(O-O-H)-C-C(=O)-O-C$^{\bullet}$
MB3D-C5H8O2	C=C-C-C(=O)-O-C
MB3OO-C5H9O4	C-C(-O-O$^{\bullet}$)-C-C(=O)-O-C
MB3OOH-C5H10O4	C-C(-O-O-H)-C-C(=O)-O-C
MB2OO-C5H9O4	C-C-C(-O-O$^{\bullet}$)-C(=O)-O-C
MBMOO-C5H9O4	C-C-C-C(=O)-O-C(-O-O$^{\bullet}$)
MB3OOH2J-C5H9O4	C-C(-O-O-H)-C$^{\bullet}$-C(=O)-O-C
MB4OO-C5H9O4	C(-O-O$^{\bullet}$)-C-C-C(=O)-O-C
MB4OOH2J-C5H9O4	C(-O-O-H)-C-C$^{\bullet}$-C(=O)-O-C
MB4OOH-C5H10O4	C(-O-O-H)-C-C-C(=O)-O-C
MB4OOH3J-C5H9O4	C(-O-O-H)-C$^{\bullet}$-C-C(=O)-O-C
MB4OOHMJ-C5H9O4	C(-O-O-H)-C-C-C(=O)-O-C$^{\bullet}$
MBMOOH-C5H10O4	C-C-C-C(=O)-O-C(-O-O-H)
MBMOOH3J-C5H9O4	C-C$^{\bullet}$-C-C(=O)-O-C(-O-O-H)
MBMOOH4J-C5H9O4	C$^{\bullet}$-C-C-C(=O)-O-C(-O-O-H)
MBMOOH2J-C5H9O4	C-C-C$^{\bullet}$-C(=O)-O-C(-O-O-H)
MB2OOH4J-C5H9O4	C$^{\bullet}$-C-C(-O-O-H)-C(=O)-O-C
MB2OOH4O2-C5H9O6	C(-O-O$^{\bullet}$)-C-C(-O-O-H)-C(=O)-O-C
MB3OOHMO2-C5H9O6	C-C(-O-O-H)-C-C(=O)-O-C(-O-O$^{\bullet}$)
MB4OOHMO2-C5H9O6	C(-O-O-H)-C-C-C(=O)-O-C(-O-O$^{\bullet}$)
MB4OOH2O2-C5H9O6	C(-O-O-H)-C-C(-O-O$^{\bullet}$)-C(=O)-O-C
MBMOOH3O2-C5H9O6	C-C(-O-O$^{\bullet}$)-C-C(=O)-O-C(-O-O-H)
MBMOOH4O2-C5H9O6	C(-O-O$^{\bullet}$)-C-C-C(=O)-O-C(-O-O-H)
MB2OOH-C5H10O4	C-C-C(-O-O-H)-C(=O)-O-C
MBKET42-C5H8O5	C(=O)-C-C(-O-O-H)-C(=O)-O-C
MBKET3M-C5H8O5	C-C(=O)-C-C(=O)-O-C(-O-O-H)
MBKET24-C5H8O5	C(-O-O-H)-C-C(=O)-C(=O)-O-C
MBKETM4-C5H8O5	C(-O-O-H)-C-C-C(=O)-O-C(=O)
MBKET4M-C5H8O5	C(=O)-C-C-C(=O)-O-C(-O-O-H)
MB3DMOOH-C5H8O4	C=C-C-C(=O)-O-C(-O-O-H)
MBM4OOH2J-C5H9O6	C(-O-O-H)-C-C$^{\bullet}$-C(=O)-O-C(-O-O-H)
MB42OOHMJ-C5H9O6	C(-O-O-H)-C-C(-O-O-H)-C(=O)-O-C$^{\bullet}$
MB24OOHMJ-C5H9O6	C(-O-O-H)-C-C(-O-O-H)-C(=O)-O-C$^{\bullet}$
MB3D2OOH-C5H8O4	C=C-C(-O-O-H)-C(=O)-O-C
MB3MOOH2J-C5H9O6	C-C(-O-O-H)-C$^{\bullet}$-C(=O)-O-C(-O-O-H)
MB3MOOH4J-C5H9O6	C$^{\bullet}$-C(-O-O-H)-C-C(=O)-O-C(-O-O-H)
MPMDO2D-C4H4O3	C-C=C(=O)-O-C(=O)
MPMJDO2D-C4H3O3	C-C=O-C(=O)-O-C$^{\bullet}$(=O)
MECY2OM-C3H4O3[1]	C(-O-)-C(=O)-O-C(-O-)
MBCY4OM-C5H8O3[1]	C(-O-)-C-C-C(=O)-O-C(-O-)
MBCY3O2-C5H8O3[1]	C-C(-O-)-C(-O-)-C(=O)-O-C
MBCY4O3-C5H8O3[1]	C(-O-)-C(-O-)-C-C(=O)-O-C
MBCY4O2-C5H8O3[1]	C(-O-)-C-C(-O-)-C(=O)-O-C
MBCY2OM-C5H8O3[1]	C-C-C(-O-)-C(=O)-O-C(-O-)
MBCY3OM-C5H8O3[1]	C-C(-O-)-C-C(=O)-O-C(-O-)
MMCYMOO1-C2H2O4[1]	C(-O-)(=O)-O-C(-O-)

[1]Species with the letters "cy" in their name are cyclic ether species. Two (-O-) symbols indicates that the same O atom is bonded with two C atoms.

References

[1] K. Narayanaswamy, P. Pepiot, and H. Pitsch. A chemical mechanism for low to high temperature oxidation of n-dodecane as a component of transportation fuel surrogates. *Combustion and Flame*, 161(4):866–884, 2014.

[2] Lam K Huynh and Angela Violi. Thermal decomposition of methyl butanoate: Ab initio study of a biodiesel fuel surrogate. *The Journal of organic chemistry*, 73(1):94–101, 2008.

[3] S. Dooley, H. J. Curran, and J. M. Simmie. Autoignition measurements and a validated kinetic model for the biodiesel surrogate, methyl butanoate. *Combustion and Flame*, 153(1):2–32, 2008.

[4] P. Pepiot-Desjardins and H. Pitsch. An efficient error-propagation-based reduction method for large chemical kinetic mechanisms. *Combustion and Flame*, 154(1-2):67–81, 2008.

[5] Jorge Mendes, Chong-Wen Zhou, and Henry J Curran. Theoretical and kinetic study of the hydrogen atom abstraction reactions of esters with ho2 radicals. *The Journal of Physical Chemistry A*, 117(51):14006–14018, 2013.

[6] Bin Yang, Charles K Westbrook, Terrill A Cool, Nils Hansen, and Katharina Kohse-Höinghaus. Fuel-specific influences on the composition of reaction intermediates in premixed flames of three c5h10o2 ester isomers. *Physical Chemistry Chemical Physics*, 13(15):6901–6913, 2011.

[7] Sandro Gaïl, Murray J Thomson, S Mani Sarathy, Sajid A Syed, Philippe Dagaut, Pascal Diévart, Anthony J Marchese, and Frederick L Dryer. A wide-ranging kinetic modeling study of methyl butanoate combustion. *Proceedings of the Combustion Institute*, 31(1):305–311, 2007.

[8] Edward R Ritter. Therm: A computer code for estimating thermodynamic properties for species important to combustion and reaction modeling. *Journal of chemical information and computer sciences*, 31(3):400–408, 1991.

[9] Release CHEMKIN-PRO. 15112, reaction design. *Inc., San Diego, CA*, 2011.

[10] H. Pitsch and M. Bollig. Flamemaster, a computer code for homogeneous and one-dimensional laminar flame calculations. *Institut fur Technische Mechanik, RWTH Aachen*, 1993.

[11] S. Gaïl, S. M. Sarathy, M. J. Thomson, P. Diévart, and P. Dagaut. Experimental and chemical kinetic modeling study of small methyl esters oxidation: Methyl (e)-2-butenoate and methyl butanoate. *Combustion and Flame*, 155(4):635–650, 2008.

[12] Anthony J Marchese, Michele Angioletti, and Frederick L Dryer. Flow reactor studies of surrogate biodiesel fuels. In *Proceedings of the 30th International Symposium on Combustion*, pages 25–30, 2004.

[13] S. S. Vasu, D. F. Davidson, Z. Hong, V. Vasudevan, and R. K. Hanson. n-dodecane oxidation at high-pressures: Measurements of ignition delay times and OH concentration time-histories. *Proceedings of the Combustion Institute*, 32(1):173–180, 2009.

[14] C. Ji, E. Dames, Y. L. Wang, H. Wang, and F. N. Egolfopoulos. Propagation and extinction of premixed C5–C12 n-alkane flames. *Combustion and Flame*, 157(2):277–287, 2010.